NON-PLANAR 3D PRINTED ELEMENTS ON TEXTILE SUBSTRATE USING A FUSED FILAMENT FABRICATION 3D PRINTER

Dominik Muenks*, Luca Eckelmann, Yordan Kyosev

Chair of Development and Assembly of Textile Products, Institute of Textile Machinery and High Performance Material Technology (ITM),

Technische Universitt Dresden, Hohe Strae 6, 01062 Dresden, Germany

*Corresponding author. E-mail: dominik.muenks@tu-dresden.de

Abstract:

Adhesion between additively printed elements on textiles is one of the most important quality characteristics. Applied elements must form very good adhesion with the textile substrate in order to produce functional textiles. The request for non-planar printing directly on textiles is growing, especially in the fields of orthopaedic engineering and protective clothing. This new printing technique can open up new areas of application. For such a production of non-planar elements on textiles, new test methods have to be developed, as the current adhesion tests (180° peel test) are not applicable to non-planar prints on textiles. For non-planar additive printing on textiles, a cylindrical print bed for a fused filament fabrication printer was developed and modified accordingly in the first step. In the next step, a new measurement method was developed to investigate the adhesion between the textile and the non-planar three-dimensional-printed element. The study shows the challenges and the adhesion differences of non-planar printed objects on pre-stretched textiles on a cylindrical print bed. Several factors influencing adhesion were identified. The alignment of the printing nozzle to the textile substrate is the key factor influencing adhesion. The alignment also has a significant influence on the visual print quality.

Keywords:

Non-planar, adhesion, print bed, FFF, additive manufacturing, textile, planar

1. Introduction

Additive printing technology is increasingly establishing itself in the textile and apparel industry. The fast-moving fashion industry has also recognized the advantages of three-dimensional (3D) printing technology for itself. Textile knee bandages and tight-fitting garments or components with additively printed protective elements are current application examples. The development of additively manufactured protective elements to reduce abrasion and wear of textile surfaces in stressed areas is the aim of this study. Abrasion protection structures with shock absorption properties were designed for high-stress areas (knee, elbow and/or shoulder areas) and additively manufactured on the textile [1-3]. In the area of combining textile materials with additive manufacturing, however, development activities are limited either to the production of composite components (short or continuous fibre reinforcement) or to the printing of textile surfaces in the planar direction. In principle, the application of additively manufactured elements to flat textiles is possible and versatile in terms of the products to be manufactured, enabling new functional garments [4,5]. Textiles and stiff additively printed elements are nowadays produced in one planar direction and only then joined together by suitable fabrication (cutting) or by reshaping (stretching) of the fabric.

However, the textile sector faces challenges in high-quality manufacturing when using additive printing technology. The adhesion between the textile and the thermoplastic polymer (filament) to be applied in the fused filament fabrication (FFF) printing process is one of the most decisive factors. The

additive printing process must be adjusted accordingly between the printing technology and the textile. The influencing parameters for sufficient adhesion between the element to be printed and the textile are many and varied, with adhesion being influenced by the filament type, viscosity of the molten filament, z-offset and the pore size of the textile [6–8]. Further important parameters that have an influence on adhesion are the print bed and the print temperature [9–11].

The additive manufacturing process is based on a basically identical sequence of operations. A component is built up layer by layer, starting with the first, lowest layer. The component geometry is created by adding material. This makes it possible to manufacture highly complex geometries in a cost- and time-efficient manner, since the component shape is not dependent on the tool shape, as is the case, for example, with casting or lathe technologies [12]. Furthermore, additive manufacturing offers a high degree of design freedom. Although colloquially referred to as 3D printing, it is more of a 2.5D print, as a 3D structure is generated by stacking 2D layers [13].

Printing on pre-formed, non-planar materials is possible using a special 3D printing technology. The technology of non-planar printing allows direct application on curved objects. This would eliminate additional fabrication steps and save costs.

A non-planar print path is a print path that can be curved in several axes in space. As non-planar 3D printing increases design freedom in additive manufacturing, this technology is useful for the majority of industries. One way to print curved



components is to use a curved print bed, such as the one used in this study. A curved print bed allows printing on pre-curved surfaces, thus new geometries are possible and especially in combination with textiles new functional textiles are possible. These combinations make it possible, for example, to manufacture garments for personal protection with partial reinforcements on flexible substrates or to produce highly customizable support structures for the medical sector (orthoses) [14,15].

In summary, a high research effort is being made on additive 3D printing technologies and the redesign of new functional textiles. However, additive built on textiles has always been reduced to 2D in-plane application. Additive printing on curved contours with pre-tensioned textiles to produce customized structures (e.g. protectors, orthotics, abrasion protection) is so far a new method of manufacturing in this field. The application of curved elements to tensioned textiles is a new manufacturing field and therefore existing norms and testing standards are not or only partially applicable.

For this reason, this study deals with the non-planar printing process on textile surfaces. For implementation, an FFF printer is modified. By means of a controlled cylindrical print bed, constant curved elements can be printed. The conversion is explained in more detail in the first part of the study. The cylindrical print bed allows a textile to be stretched in order to carry out non-planar printing on it. For planar printing on textile surfaces, there are few experience reports and investigations available, but not for non-planar printing on textiles. Therefore, the adhesion between non-planar printed elements and textile is investigated. In the course of the investigation, it becomes clear that the adhesion on non-planar textiles cannot be applied by means of existing standards, such as DIN EN 28510-1, 53530 and 8510-2. A new test method for the adhesion of non-planar printed elements to textiles has to be developed and will be presented.

2. Methods

2.1. Changeover to cylindrical print bed for non-planar printing

An Original Prusa i3 MK3S FFF printer was used for the study. The printer and slicer is an open-source system. Structurally, the individual components such as the circuit board, stepper motors for x/y/z and printing plate are easily accessible and allow structural modification. Since the slicer (PrusaSlicer version 2.2.) generates a common and usual G-code, it can also be adapted.

First, the diameter of the cylindrical print bed must be defined. The diameter of the cylindrical print bed depends on the original print bed dimensions. According to the manufacturer, the print build space size is $250 \text{ mm} \times 210 \text{ mm} \times 210 \text{ mm} (x/y/z)$ [16].

The diameter gives the curvature K of the cylinder, the circumference u and the maximum print height. A diameter d_z of 100 mm was selected for the cylindrical print bed. This results in a circumference u of around 314 mm. The rotational centre of

the print bed is 60 mm (radius and distance between original print plat and cylindrical print bed). With a cylinder radius of 50 mm, the maximum print height is 10 mm (distance between planar print bed and the cylindrical print bed).

In the Prusa printer's conventional planar print bed, three individual NEMA (National Electrical Manufacturers Association) stepper motors are used to drive all three axes (x/y/z). The motion of the NEMA 17 stepper motor, responsible for the y-direction, is transmitted from a pinion to a belt and converts the rotational motion into a translational motion. The stepper motor has a step angle φ of 1.8°, resulting in a step count n of 200 for one revolution. The pitch circle diameter of the pinion is $d_{\rm R}=10.19\,{\rm mm}$. This results in a step size (rotatory) $S_{\rm R}$ of 0.16 mm. This means that the print bed moves 0.16 mm in the y-direction with a step angle of 1.8°.

For a defined cylindrical diameter d_z of 100 mm, the step size (cylindrical) changes and S_z is 1.57 mm. Therefore, the step size $S_R < S_Z$. The larger step size means that components do not have the correct dimensioning and the relation between extruded filament and motion is not correct. Thus, in addition to the wrong dimensioning, an undersupply of filament would come during the printing process. Thus, a direct drive of the axis of the cylindrical print bed is not possible. A corresponding transmission is required.

The cylindrical print bed with a d_z of 100 mm was designed with internal gearing. A NEMA 17 stepper motor was also selected for the power supply. This drives an externally toothed pinion and transmits the movement to the cylindrical print bed. A straight-toothed involute gear is selected as the gearing. The gear pair is adapted to the diameter of the cylindrical print bed, and only in this combination can a correct step width be achieved at the height of the print bed. The schematic design is shown in Figure 1.

Step count *n* is calculated by:

$$n = \frac{360^{\circ}}{\varphi}.\tag{1}$$

Step width S is calculated by:

$$S = \frac{d}{2} \times \frac{\pi}{180} \varphi . \tag{2}$$

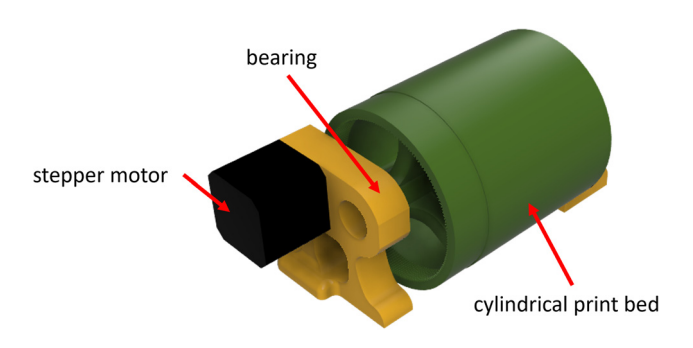


Figure 1. Schematic drawing of the cylindrical print bed.

The components (holder, cylindrical print bed, pinion) were also printed with the Prusa printer on the conventional planar printing plate. The components should have high strength with low flexibility and also have minimal shrinkage. For this reason, polylactic acid (PLA; NatureWorks LLC) was chosen as the printing filament [17]. For the fabrication of the cylindrical print bed as well as for the fabrication of the test specimens, PLA was distributed by Prusa Research a.s.. The other printing parameters are listed in Table 1.

The printed parts were assembled accordingly and the axis of the cylindrical print bed was equipped with bearings. For better fixation, magnets were installed in the holders of the construction and could thus be precisely aligned and prevented slipping during the printing process. A constant and repeatable placement of the construction was achieved by markings on the planar print bed. By using a designed holding device for the planar print bed and thus for the cylindrical print bed, it was always possible to ensure the same positioning. The nozzle was thus always at the vertex of the cylindrical print bed. The movement of the planar stepper motor, responsible for the x-axis movement, was deactivated and replaced by the cylindrical movement of the NEMA stepper motor. Figure 2 shows the overall setup and positioning.

2.2. Adhesion measurement between textile and printed elements

A common method for testing the adhesion between 3D printed elements is a so-called peel test. There are various peel tests

Table 1. Printing parameters for the production of the cylindrical printing bed and its components

| Printing parameters | | |
|----------------------------|------|--|
| Extruder temperature (°C) | 200 | |
| Print bed temperature (°C) | 60 | |
| Layer height (mm) | 0.15 | |
| Infill (%) | 10 | |
| Nozzle diameter (mm) | 0.4 | |

for measuring adhesion, such as the standards DIN EN 28510-1, 53530 and 8510-2. Depending on the standard, the test differs in its scope of application and its execution [18-20]. A test standard for printed additive elements on textiles does not yet exist. Therefore, testing can only be carried out on the basis of the standards. DIN EN ISO 8510-2 was used for the investigation in these studies [21]. The standard is used for a 180° peel test. For this purpose, a bar-like structure of a certain width and height is printed on the textile surface. The printed PLA specimens on textile in this study have dimensions of 120 mm \times 50 mm \times 2 mm (x/y/z) and were tested with a ZwickRoell Z2.5. The load cell used with this has a maximum recordable force of 2500 N. A schematic diagram of the planar 180° peel test is shown in Figure 3. This test method, however, is not suitable for testing printed, curved (non-planar) and rigid joining parts on textiles. Due to the curvature of the rigid joining part, a peel test using the 180° method is not possible, as the rigid joining part is in the way of the pull-off of the flexible joining part. For this reason, an adapted test method had to be developed.

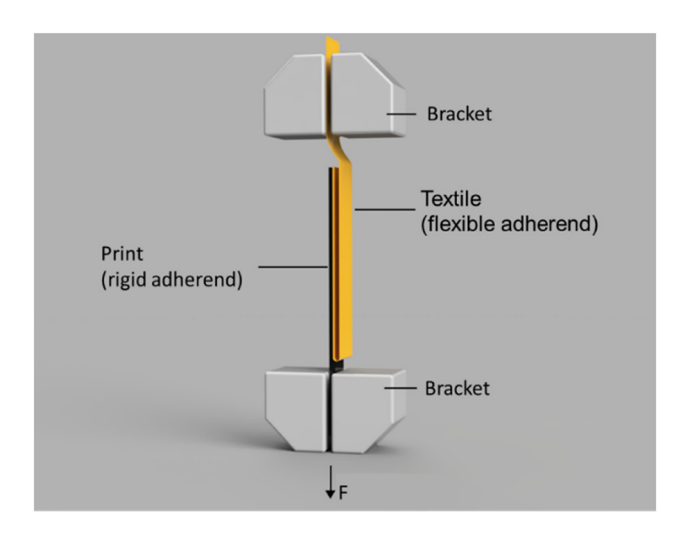


Figure 3. Schematic drawing of the 180° peel test according to DIN 8510.2

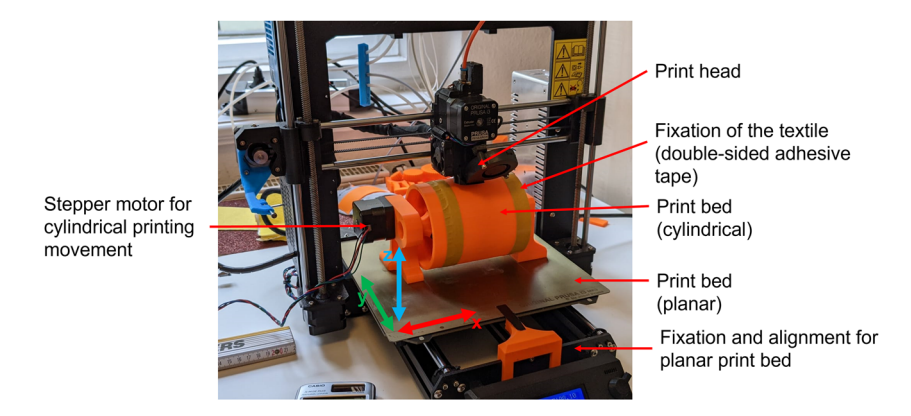
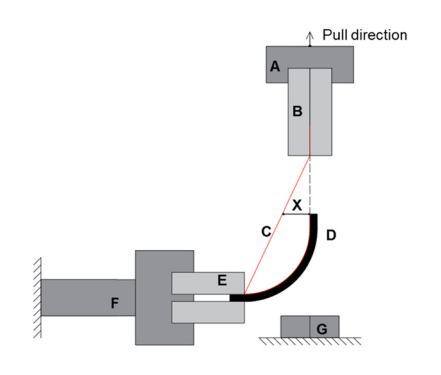


Figure 2. Realized modification to the cylindrical print bed.

2.3. Development of a method for measuring adhesion on curved textile surfaces

To test printed and curved elements, a clamp had to be rotated 90° so that a peel test could be performed without the parts getting in each other's way.

Figure 4 shows a simplified schematic of the test setup, in more detail the action range of the peel test for non-planar specimens. It must be ensured that the distance X between the flexible joining part and the PLA sample is greater than zero, so that there is no collision and no unwanted friction points or forces between the textile and the PLA sample during the test. Furthermore, it must be ensured that the last area of the peel test, that is the contact surface between the textile and the PLA sample is in alignment with the clamping area of clamp 1 (B). At the end of the peel test, the textile is thus peeled off perpendicular to clamp 2 (E), or parallel to the end of the PLA sample. The last section is thus peeled off like a planar specimen; the peeling direction is in one plane with the contact surface between textile and PLA specimen.



- A Load cell
- B Clamp
- C Textile sample
- D Non-planar print
- E Clamp
- F Support frame for non-planar
- G Support frame for planar

X - distance between textile and from non-planar print

Figure 4. Schematic layout of the equipment for measuring the adhesion between textile and imprinted elements.

For the peel test (according to DIN 8510-2) of the planar printed specimens, the holder frame is dismantled and clamp 2 (E) is mounted on the actual holder (G) of the tensile testing machine. The planar printed specimen is now fixed with clamp 2 (E), the textile is fixed in clamp 1 (B) and the textile is pulled off upwards, analogously as schematically shown in Figure 3. Figure 5 shows the setup and testing in the laboratory.

2.4. Specimen preparation for peel tests

A cotton fabric (twill weave, sanforized, with a 185 g/m² fibre area weight) was selected as the textile printing substrate. The choice of fabric was based on previous tests and literature research, which showed that PLA prints well on textile surfaces [22], as well as the combination cotton–PLA proves to be a good combination [23].

For the peel test, three different sample types with three samples each are prepared. A PLA was also used to print on textile:

- Specimen type 1: planar manufactured specimens specimen identification P
- Specimen type 2: non-planar specimens on the constructed cylindrical print bed – specimen identification NP
- Specimen type 3: non-planar manufactured specimens on the constructed cylindrical print bed with an additional shift of the nozzle by 10 mm in the y-direction. Thus, the nozzle does not print directly on the apex of the cylindrical print bed, but with the same offset to the textile – specimen identification NPV.

Figure 6 shows the schematic diagram of the nozzle placement of sample types 2 and 3.

Figure 7 shows the three printed specimen types. Planar printed specimens (P) are identified as P1 to P3, non-planar

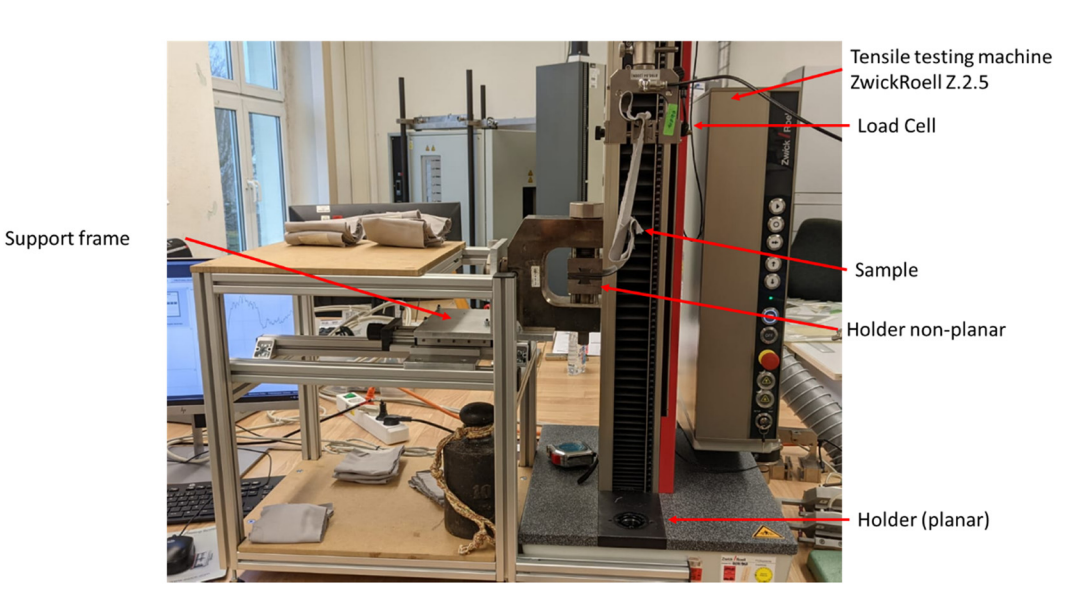


Figure 5. Realized measuring equipment for measuring the adhesion of non-planar pressure elements on textile.

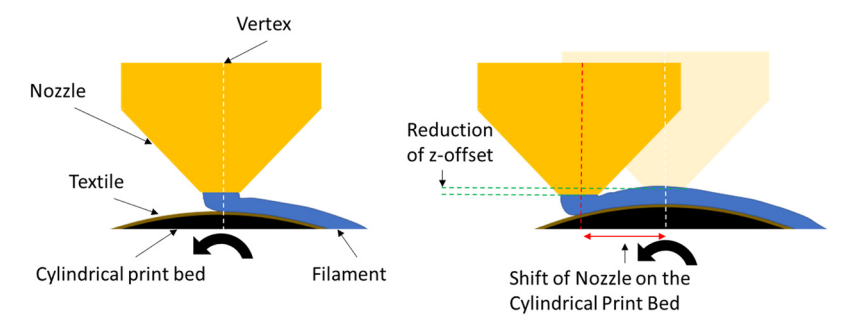


Figure 6. Left: schematic representation of the nozzle arrangement of sample type 2 (NP). Right: schematic representation of the nozzle arrangement with a shift – sample type 3 (NPV).

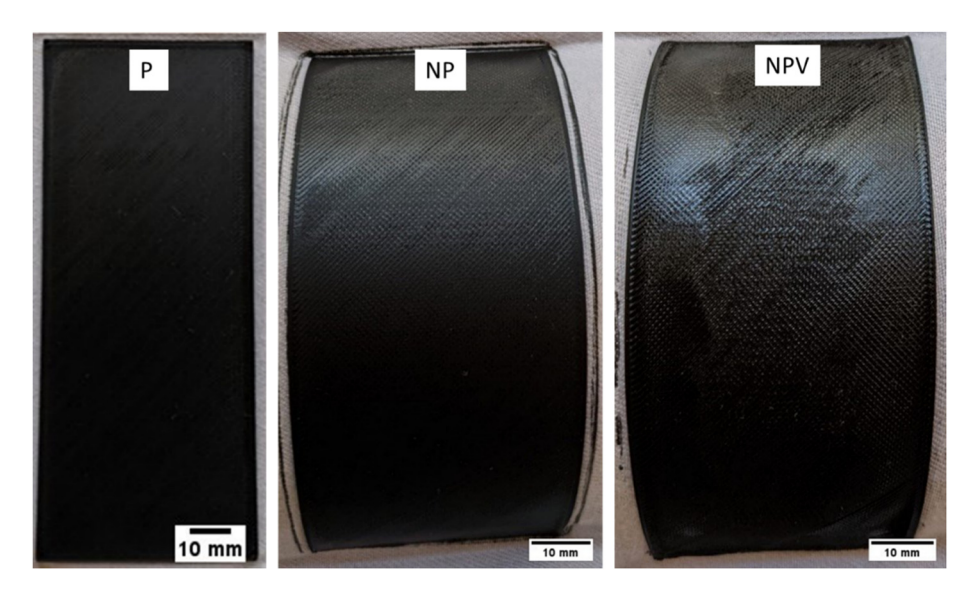


Figure 7. Printed samples on textile – planar sample (P), non-planar sample (NP) and non-planar sample with shift (NPV).

printed specimens (NP) as NP1 to NP3 and non-planar offset printed specimens (NPV) as NPV1 to NPV3.

For printing on textile, the z offset (distance between print head and textile) must be adjusted. For this purpose, the offset was increased by $0.2 \, \text{mm}$ (z direction). The offset was set to the same value for all sample types. All other print parameters are listed in Table 2.

3. Results and discussion

3.1. Visual observation

When the three different printed sample types are visually examined, it is noticeable that there are qualitative differences on the top layer. The samples with the shift (NPV) show an uneven surface compared to the other samples. As can be seen in Figure 7, the non-planar print with shift (NPV) has an uneven and partially roughened surface. The uneven surface can be explained by the fact that the nozzle has a different distance to the cylindrical print bed. Towards the vertex, the distance is smaller than that towards the opposite side. Figure 8 shows the different nozzle distance to the

Table 2. Print parameters for the preparation of the specimens

| Print parameters | |
|----------------------------|--------------|
| Extruder temperature (°C) | 220 |
| Print bed temperature (°C) | Not possible |
| Layer height (mm) | 0.15 |
| Nozzle diameter (mm) | 0.4 |
| Print speed (mm/s) | 50 |
| Sample dimensions (mm) | |
| in x | 120 |
| in y | 50 |
| in z | 2 |
| Infill | No |

cylindrical print bed of the nozzle. If the nozzle is shifted and the angle to the cylindrical print bed is not adjusted, a critical point is created. The different distance to the print bed causes printing problems, as shown above in figure 7 NPV. It should be mentioned again that the distance between the cylindrical print bed and the nozzle was kept the same. For the NPV samples, the nozzle was shifted downwards by 1 mm. For optimisation,

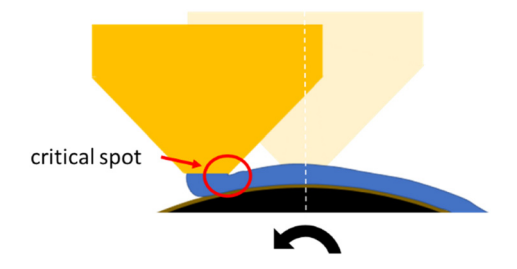


Figure 8. Possible critical point causing an inaccurate printing surface.

the angle of the nozzle would have to be adjusted and it would have to be perpendicular to the cylindrical print bed to avoid the critical point and achieve optimised print results.

Figure 9 shows another irregularity that occurs during nonplanar printing. The print object shown was printed in different gradations (gradation 1 with 10 mm to gradation 4 with 40 mm). As the print height increases, it is noticeable that the individual lanes no longer bond sufficiently to each other. At 40 mm

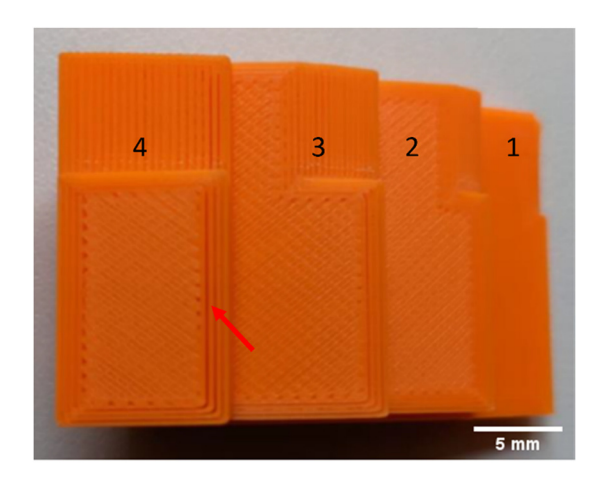


Figure 9. Test print object with different gradations (1-10 mm, 2-20 mm, 3-30 mm, and 4-40 mm) with visible print lanes that are not connected at gradation 4.

(gradation 4), the print webs are no longer connected to each other, gaps appear between the filament layers. As a result, the printed object loses stability. This fact occurs with increasing print height and thus increasing radius to the cylindrical print.

Figure 10 shows the change in step width as the layer height to be printed increases for different cylindrical print set radii.

Step width for the number of layers to be printed is given by:

$$S_{L_c} = (r_z + L_c \times L_h) \times \varphi. \tag{3}$$

The layer height $(L_{\rm h})$ is always constant; it is the height (z-height) that the printer adds at the next layer, in this case it is 0.15 mm. The number of layers $(L_{\rm c})$ increases during printing, from 1 layer to 100 layers. Different radii were chosen for the cylindrical print bed $(r_{\rm z})$ to show the influence on the step size. The radian φ remains constant in all calculations.

In Figure 10, we can observe that the appearance shown in Figure 9 is less for smaller radii than for larger radii. As the number of layers (L_c) increases, the step size increases. This can also be seen in Figure 9. In gradation 1, the paths are still close together, and in gradation 4, they are clearly printed apart.

In the printed non-planar test prints (NP and NPV seen in Figure 7), the separating layers occurred but was hardly visible due to the low number of layers, in that case 13 printed layers. Therefore, it can be assumed that this has no influence on the adhesion to the textile, since it is mainly the first layer that adheres to the textile.

3.2. Evaluation of the peel tests

The 180° peel test and the method introduced were evaluated according to the DIN 8510-2 standard. Chapter 8 of the standard specifies that the average peel forces must be determined in Newtons. At least a peel length of 100 mm must be evaluated, with the first 25 mm being discarded. In the study, the

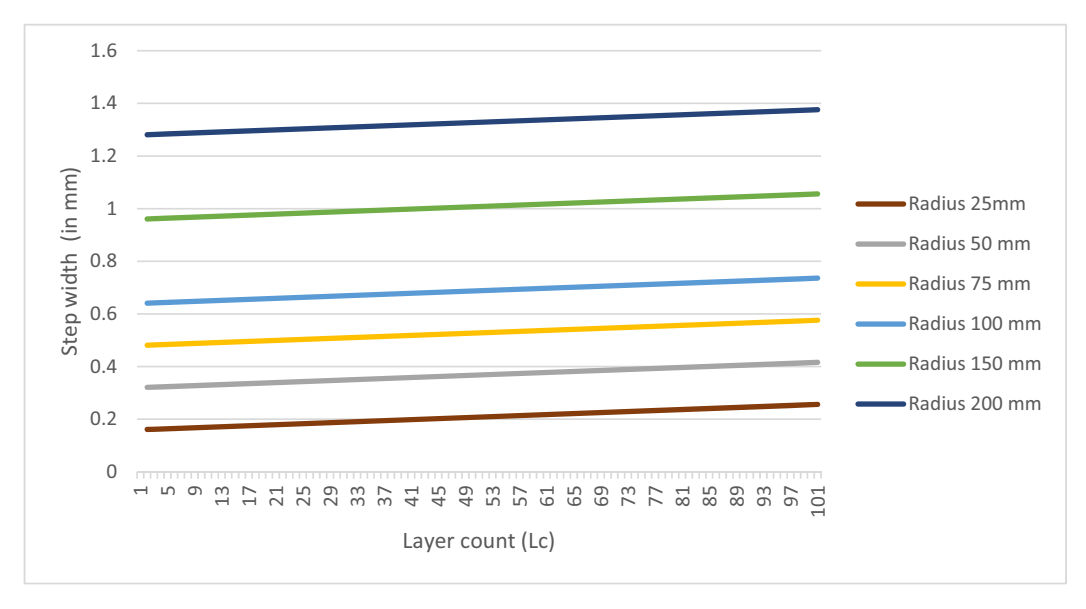


Figure 10. Step size for different cylindrical pressure beds with increasing layer height.

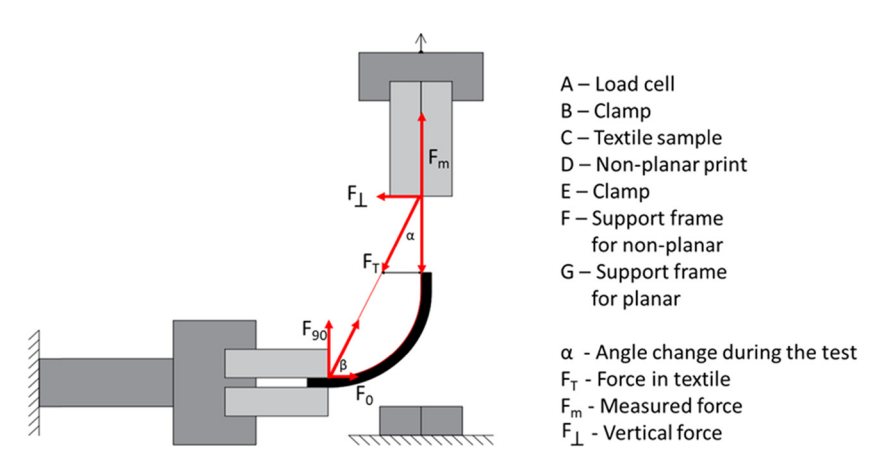


Figure 11. Schematic illustration of the force curves during non-planar measurement.

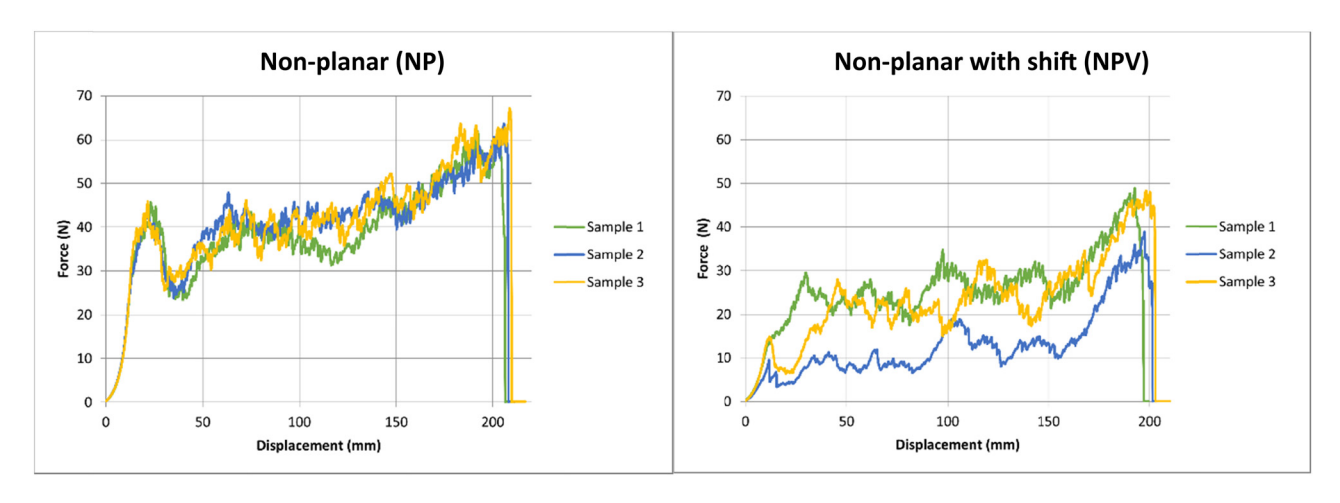


Figure 12. Peel test results of all three sample types – over the whole recorded peel test.

starting point of the evaluation was set to be 25 mm after the first peak, and then 125 mm of precipitation length was evaluated. Figures 12 and 13 show the entire measured range.

Figure 11 shows the force characteristics during the developed non-planar peel test. It should be noted that the measured forces change during the non-planar peel test due to the angular change of α and β . Therefore, the results are not

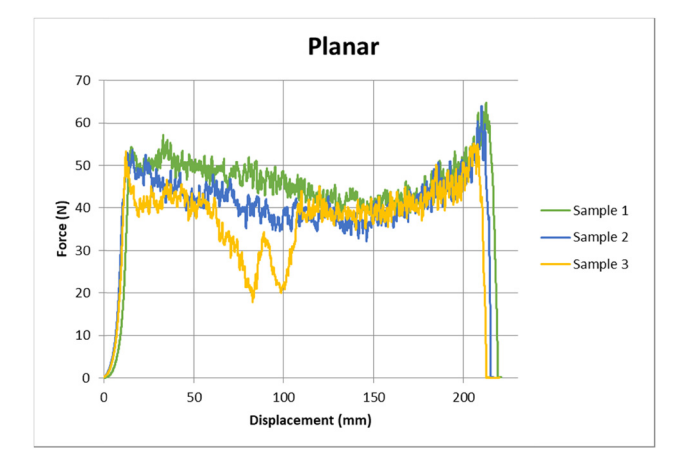


Figure 13. Planar peel test results – over the whole recorded peel test.

comparable with other cylindrical radii. It can be noted that this measurement method and the results depend on the geometry and the radius. Therefore, comparability with the 180° peel test is also not possible. However, since the adhesion influence of a shift of the printing nozzle on a cylindrical printing bed with stretched textile is examined and the radius of the printing bed is not changed, the results can be compared with each other.

Looking at Figure 12 of the non-planar measurement (NP), it can be noted that all three measurements are very similar in their course and all measurements are very close to each other. It can be assumed that these results are well reproducible. If, on the other hand, the non-planar measurement is considered with a shift of the nozzle, the courses of the three measurements are very different. Also the forces vary very much – steep increases and decreases. In the NPV force measurements, it can be stated that the adhesion is very different within a sample, but also in different measurements. A process reliability is not given, whereas it is possible to speak of process reliability with the NP.

If the planar measurement (P) (Figure 13) is taken into account, differences in the force measurement curves can also be seen here. These are not as uniform in their course as in the NP measurement. It is interesting to compare the two measurements of planar (P) and non-planar (NP), because it could be assumed that the adhesion of the NP pressures decreases due

to the modification of the cylindrical print bed, orientation and gear drive, or the progression is irregular in the NP measurement, which is not the case. This shows that the cylindrical print bed allows uniform adhesion, as long as the nozzle is placed vertically on the textile.

Figure 14 shows the average maximum peel forces for all specimen types. The planar specimens were tested using the 180° peel test (Figure 3) and the non-planar specimens, as well as those with offsets, were tested using the method presented (Figure 4). As already mentioned, these are two different measuring methods and therefore cannot be compared with each other. Only, the non-planar measurement method and its results, by using the same print bed radius, can be compared. The planar test must be considered separately.

The maximum force in the 180° peel test for the planar specimens is 54.7 N (standard deviation of 1.7). For the non-planar specimens, the maximum force according to the method presented is 49.2 N (standard deviation of 2.1). The maximum force for the non-planar specimens with a shift is significantly lower. Here, it is only 28.7 N (standard deviation of 6.9). The non-planar samples with a shift (NPV) exhibit half as much adhesion between the textile and the imprint, compared to NP. The standard deviation is also very large for non-planar (NPV) printing.

At this point, it can be stated that if the nozzle is not printed vertically (apex) on the textile (on the planar base), there is a significant loss of adhesion. In addition, the print quality decreases significantly with an offset, as can be seen in Figure 7.

4. Conclusions and recommendations

After analysing and discussing all experimental results, the following conclusions can be drawn:

 Additively applied elements can be printed not only on planar textiles but also on non-planar stretched textiles. Due to the constructed cylindrical print bed, it was possible to print non-planar textiles. The orientation of the nozzle is important

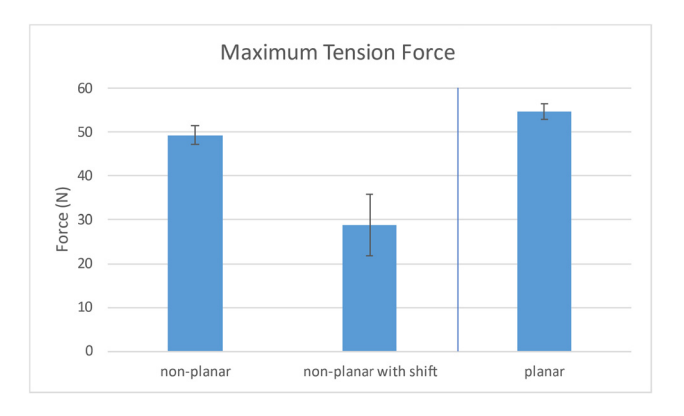


Figure 14. Maximum tensile force of all three specimen types – non-planar and offset specimens were tested according to the presented methodology and the planar specimens were tested according to the 180° peel test.

http://www.autexrj.com/

and must always be set on the vertex. If there is a shift, the adhesion decreases significantly. With a shift of 10 mm of the nozzle to the vertex with constant z-offset, the adhesion between textile and print object is reduced by around half.

- When using multi-axis printers on textiles in the future, it is important to ensure that there is no shift from the apex and that the nozzle is perpendicular to the substrate.
- A new test device had to be developed for measuring adhesion, since curved printed textiles cannot be tested with the previous standards. However, this measurement method is only applicable and comparable for printing on the same radius of the cylindrical print bed. A possible future improvement is a video recording during the test and subsequent observation of the angle change. From this, the force changes during the measurement could also be analysed.
- The print quality of non-planar printing with an offset (NPV) is lower compared to planar or non-planar printing. This is due to the angle of the print nozzle to the print bed (Figure 8). This can be improved by aligning the nozzle vertically to the print bed, which was not possible with the current printer, due to the rigid axes.
- Due to the layered structure of print objects, it is noticeable that the lanes no longer connect sufficiently with each other. As a result, the printed object loses stability. This effect occurs with increasing print height and thus increasing radius of the cylindrical print object. However, this could be improved by adapting the G-code. The adaptation can ensure that the individual filament webs are still connected to each other as the radius increases.
- A heated print bed temperature has a positive effect on adhesion [22,24]. In this study, the print bed was not preheated, so it can be assumed that a heated print bed could improve adhesion. This should be taken into account in further development of the cylindrical print bed.

Acknowledgements: We would like to thank for the award at the Autex Conference 2022 and the funding for this publication.

Funding information: The IGF research project 21622 BR of the Forschungsvereinigung Forschungskuratorium Textil e. V. is funded through the AiF within the program for supporting the "Industriellen Gemeinschaftsforschung (IGF)" from funds of the Federal Ministry for Economic Affairs and Climate Action on the basis of a decision by the German Bundestag.

Conflict of interest: Authors state no conflict of interest.

References

502

[1] Pröbsting, J., Günther, N. (2014). Generative fertigungsverfahren in der orthopädie-technik. Orthopädie Technik, 1, 1–4.

- [2] Glogowsky, A., Korger, M., Sanduloff, S., Steinem, C., Huysman, S., Ernst, M., et al. (2020). 3D printed structures for customized protective elements: soft prints with tough requirements. 3. European Industry and Research Exchange on Technical Textiles for Health, Medical and Sport Application Online Conference.
- [3] Sächsisches Textilforschungsinstitut e.V. (2020). 3Dgedruckter Abriebschutz mit kompressiblen Eigenschaften. https://www.stfi.de/aktuelles/meldungen/meldungen-detailseite/3d-gedruckter-abriebschutz-mit-kompressiblen-eigenschaften. Accessed 3 September 2020.
- [4] Stapleton, S. E., Kaufmann, D., Krieger, H., Schenk, J., Gries, T., Schmelzeisen, D. (2019). Finite element modeling to predict the steady-state structural behavior of 4D textiles. Textile Research Journal, 89(17), 3484–3498. doi: 10.1177/0040517518811948.
- [5] Sitotaw, D. B., Ahrendt, D., Kyosev, Y., Kabish, A. K. (2020). Additive manufacturing and textiles—state-of-the-art. Applied Sciences, 10(15), 5033. doi: 10.3390/app10155033.
- [6] Kozior, T., Döpke, C., Grimmelsmann, N., Juhász Junger, I., Ehrmann, A. (2018). Influence of fabric pretreatment on adhesion of three-dimensional printed material on textile substrates. Advances in Mechanical Engineering, 10(8), 168781401879231. doi: 10.1177/1687814018792316.
- [7] Unger, L., Scheideler, M., Meyer, P., Harland, J., Gorzen, A., Wortmann, M, et al. (2018). Increasing adhesion of 3D printing on textile fabrics by polymer coating. Tekstilec, 61(4), 265–271. doi: 10.14502/Tekstilec2018.61.265-271.
- [8] Spahiu, T., Grimmelsmann, N., Ehrmann, A., Piperi, E., Shehi, E. (2017). Effect of 3D printing on textile fabric. Engineering and Entrepreneurship, Tirana, Albania.
- [9] Döpke, C., Grimmelsmann, N., Ehrmann, A. (2017). 3D printing on knitted fabrics. Melliand International, 23, 97–98.
- [10] Grimmelsmann, N., Kreuziger, M., Korger, M., Meissner, H., Ehrmann, A. (2018). Adhesion of 3D printed material on textile substrates. Rapid Prototyping Journal, 24(1), 166–170. doi: 10.1108/RPJ-05-2016-0086.
- [11] Malengier, B., Hertleer, C., van Langenhove, L., Cardon, L. (2017). 3D printing on textiles: testing of adhesion. International Conference on Intelligent Textiles and Mass Customisation.
- [12] Gebhardt, A. (2016). Additive Fertigungsverfahren. additive manufacturing und 3D-Drucken für Prototyping tooling Produktion (5th ed.). Hanser (München).
- [13] O'Connell, J. (31 January, 2021). Non-planar 3D printing: all you need to know. All3DP. https://all3dp.com/2/non-planar-3d-printing-simply-explained/ (Accessed 30 May 2022).
- [14] Ahrendt, D., Romero Karam, A. (2020). Development of a computer-aided engineering-supported process for the manufacturing of customized orthopaedic devices by three-dimensional printing onto textile surfaces. Journal of Engineered Fibers and Fabrics, 15(15). doi: 10.1177/ 1558925020917627.

- [15] Ahrendt, D. (2022). CAE-Prozesskette für individuelle orthopädische Hilfsmittel. Kombination von faserverstärkter additiver Fertigung und textilen Materialien (1st ed.). Springer eBook Collection. Springer Fachmedien Wiesbaden, Springer Vieweg (Wiesbaden) Imprint.
- [16] Original Prusa i3 MK3S + kit | Original Prusa 3D printers directly from Josef Prusa. https://www.prusa3d.com/product/original-prusa-i3-mk3s-kit-3/ (Accessed 4 November 2022).
- [17] Letcher, T., Waytashek, M. (2015). Material property testing of 3D-printed specimen in PLA on an entry-level 3D printer. Proceedings of the ASME International Mechanical Engineering Congress and Exposition – 2014. Presented at ASME 2014 International Mechanical Engineering Congress and Exposition; November 14–20, 2014, Montreal, Quebec, Canada. ASME 2014 International Mechanical Engineering Congress and Exposition, Montreal, Quebec, Canada, 11/14/2014–11/20/2014. ASME, New York, NY. doi: 10.1115/IMECE2014-39379.
- [18] Fafenrot, S., Korger, M., Ehrmann, A. (2019). Mechanical properties of composites from textiles and three-dimensional printed materials. In: Jawaid, M., Thariq, M., Saba, N. (Eds.) Mechanical and physical testing of biocomposites, fibre-reinforced composites and hybrid composites. Woodhead Publishing Series in Composites Science and engineering. Woodhead Publishing (Duxford). pp. 409–425.
- [19] Koch, H. C., Schmelzeisen, D., Gries, T. (2021). 4D textiles made by additive manufacturing on pre-stressed textiles—an overview. Actuators, 10(2), 31. doi: 10.3390/act10020031.
- [20] Narula, A., Pastore, C. M., Schmelzeisen, D., El Basri, S., Schenk, J., Shajoo, S. (2018). Effect of knit and print parameters on peel strength of hybrid 3-D printed textiles. Journal of Textiles and Fibrous Materials, 1. doi: 10.1177/251522 1117749251.
- [21] DIN Deutsches (2010). Klebstoffe Schälprüfung für flexibel/starr geklebte Proben - Teil 2: 180-Grad-Schälversuch. Institut für Normung e.V., Beuth Verlag GmbH (Berlin) (DIN EN ISO 8510-2).
- [22] Hashemi Sanatgar, R., Campagne, C., Nierstrasz, V. (2017). Investigation of the adhesion properties of direct 3D printing of polymers and nanocomposites on textiles: Effect of FDM printing process parameters. Applied Surface Science, 403, 551–563. doi: 10.1016/j.apsusc.2017.01.112.
- [23] Pei, E., Shen, J., Watling, J. (2015). Direct 3D printing of polymers onto textiles: experimental studies and applications. Rapid Prototyping Journal, 21(5), 556–571. doi: 10.1108/RPJ-09-2014-0126.
- [24] Eutionnat-Diffo, P. A., Chen, Y., Guan, J., Cayla, A., Campagne, C., Zeng, X, et al. (2019). Stress, strain and deformation of poly-lactic acid filament deposited onto polyethylene terephthalate woven fabric through 3D printing process. Scientific Reports, 9, 14333. doi: 10.1038/ s41598-019-50832-7.

http://www.autexrj.com/